Published in final edited form as:
Biochemistry. 2013 February 19; 52(7): 1137–1148. doi:10.1021/bi3012059.

Diaryl Hydrazones as Multifunctional Inhibitors of Amyloid Self-Assembly†

Béla Török,
Department of Chemistry, University of Massachusetts Boston, 100 Morrissey Blvd. Boston, MA 02125-3393

Abha Sood,
Department of Chemistry, University of Massachusetts Boston, 100 Morrissey Blvd. Boston, MA 02125-3393

Seema Bag,
Department of Chemistry, University of Massachusetts Boston, 100 Morrissey Blvd. Boston, MA 02125-3393

Rekha Tulsan,
Department of Chemistry, University of Massachusetts Boston, 100 Morrissey Blvd. Boston, MA 02125-3393

Sanjukta Ghosh,
Department of Chemistry, University of Massachusetts Boston, 100 Morrissey Blvd. Boston, MA 02125-3393

Dmitry Borkin,
Department of Chemistry, University of Massachusetts Boston, 100 Morrissey Blvd. Boston, MA 02125-3393

Arleen R. Kennedy,
Department of Chemistry, University of Massachusetts Boston, 100 Morrissey Blvd. Boston, MA 02125-3393

Michelle Melanson,
Department of Chemistry, University of Massachusetts Boston, 100 Morrissey Blvd. Boston, MA 02125-3393

Richard Madden,
Department of Chemistry, University of Massachusetts Boston, 100 Morrissey Blvd. Boston, MA 02125-3393

Weihong Zhou,
Department of Chemistry, University of Massachusetts Boston, 100 Morrissey Blvd. Boston, MA 02125-3393

Harry LeVine III, and
Department of Cellular and Molecular Biochemistry, Center on Aging, Center for Structural Biology, University of Kentucky, 800 S. Limestone Street, Lexington, KY 40536-0230

[*]Corresponding author: Marianna Torok, Department of Chemistry, University of Massachusetts Boston, 100 Morrissey Blvd. Boston, MA 02125-3393, Tel.:(617)-287-6159 Fax:(617)-287-6030, marianna.torok@umb.edu.

SUPPORTING INFORMATION

The synthesis and spectral characterization of the hydrazones used in this study are provided. This material is available free of charge via the Internet at http://pubs.acs.org.

Marianna Török*
Department of Chemistry, University of Massachusetts Boston, 100 Morrissey Blvd. Boston, MA 02125-3393

Abstract

The design and application of an effective, new class of multifunctional small molecule inhibitors of amyloid self-assembly are described. Several compounds, based on the diaryl hydrazone scaffold were designed. Forty-four substituted derivatives of this core structure were synthesized using a variety of benzaldehydes and phenylhydrazines and were characterized. The inhibitor candidates were evaluated in multiple assays, including the inhibition of Aβ fibrillogenesis and oligomer formation and the reverse processes, the disassembly of preformed fibrils and oligomers. Since the structure of the hydrazone-based inhibitors mimic the redox features of the antioxidant resveratrol the radical scavenging effect of the compounds was evaluated by colorimetric assays against 2,2-diphenyl-lpicrylhydrazyl (DPPH) and superoxide radicals.

The hydrazone scaffold was active in all of the different assays. The structure-activity relationship revealed that the substituents on the aromatic rings had considerable effect on the overall activity of the compounds. The inhibitors showed strong activity in the fibrillogenesis inhibition and disassembly, and even greater potency in the inhibition of oligomer formation and oligomer disassembly. Supporting the quantitative fluorometric and colorimetric assays, size exclusion chromatographic studies indicated that the best compounds practically eliminated or substantially inhibited the formation of soluble, aggregated Aβ species, as well. Atomic Force Microscopy was also applied to monitor the morphology of Aβ deposits. The compounds also possessed the predicted antioxidant properties; approximately 30% of the synthesized compounds showed equal or better radical scavenging effect than resveratrol or ascorbic acid.

INTRODUCTION

The formation of misfolded, amyloid-like protein assemblies in cells and tissues is observed in many aging-related diseases such as Alzheimer's disease (AD). The major constituent of these protein aggregates in the case of AD, is the amyloid β (Aβ) peptide.[1,2] Traditionally the insoluble Aβ fibrils were proposed as one of the major causes of AD, however, more recently soluble oligomeric species of Aβ were shown to exhibit even stronger and more potent neurotoxicity.[3] While the application of small molecule fibril and oligomer formation inhibitors has been a popular treatment strategy[4] relatively few studies address the development of compounds that affect multiple toxic processes.[5,6]

Many inhibitors of Aβ self-assembly have been identified including small organic molecules, peptides, peptidomimetics and proteins.[7–9] These compounds have been categorized as anti-fibril or anti-oligomer compounds. Oligomer structures were generally detected with conformation-specific antibodies.[10–12] Peptide-based inhibitors have been frequently used to investigate the driving forces responsible for self-assembly and the π-π stacking between aromatic residues has been identified to be of primary importance,[13,14] although it is not the exclusive factor in governing amyloid formation.[15] The literature on small organic molecule inhibitors is less systematic focusing on their biopharmaceutical properties rather than their mechanism of action.[4,16,17]

Oxidative stress is believed to contribute to neurodegeneration in AD. Since *in vivo* studies indicate elevated levels of oxidative stress in the AD affected brain,[18] including antioxidant properties in the design of Aβ self-assembly inhibitory compounds appears desirable.[19,20] The precise relationship between Aβ self-assembly, neurotoxicity and oxidative stress is still somewhat unclear. Aβ and some of its derivatives generate free radicals spontaneously upon

oligomerization and fibrillogenesis, most likely with the contribution of metal ions.[21–23] Formation of free radicals during the disassembly of preformed Aβ fibrils[24] and a free radical scavenging capacity of Aβ itself has also been observed.[25] Regardless of whether oxidative stress precedes amyloid assembly or the level of reactive oxygen species (ROS) increases as a consequence of changes in the oligomeric state of Aβ, free radicals negatively affect cellular function and survival.[26,27] Optimally, small molecule agents targeting Aβ self-assembly/disassembly should not induce the formation of ROS and they should scavenge any ROS present. Dietary antioxidants, especially plant-derived polyphenols, may provide beneficial effects in AD through multiple mechanisms.[28–30] Although they can protect against the effects of ROS, most of the natural antioxidants are poor drug candidates due to a lack of metabolic stability, oral bioavailability or brain penetration.[31]

Herein, we describe the synthesis and evaluate the structure-activity relationship of a new class of multifunctional compounds that interfere with the self-assembly of Aβ into fibrils and oligomers and also are able to combat the effects of harmful free radicals. A diverse group of bis(aryl)-hydrazones were synthesized and tested in this study. While a number of useful therapeutic agents are hydrazones/hydrazines, including CNS penetrant drugs,[32] such compounds have been infrequently used in AD related studies.[33,34]

MATERIALS AND METHODS

General Information - Synthesis

The substituted hydrazines, benzaldehydes and the ^{19}F NMR reference compound $CFCl_3$ were purchased from Aldrich. DMSO(d_6) and $CDCl_3$ used as a solvent (99.8%) for the NMR studies were Cambridge Isotope Laboratories products. Other solvents used in synthesis with minimum purity of 99.5% were from Fisher. The mass spectrometric identification of the products was carried out by an Agilent 6850 gas chromatograph – 5973 mass spectrometer system (70 eV electron impact ionization) using a 30m long DB-5 column (J&W Scientific). An Agilent HPLC-MS (Series 1200 HPLC-6130 Qadrupole MS) was also used for the identification of certain compounds that appeared thermally unstable above 250 °C, the injector temperature for GC-MS. The ^{1}H, ^{13}C and ^{19}F NMR spectra were obtained on a 300 MHz superconducting Varian Gemini 300 NMR spectrometer, in DMSO(d_6) and $CDCl_3$ with tetramethylsilane and $CFCl_3$ as internal standards.

Synthesis of 1-benzylidene-2-phenylhydrazine—In a 15 mL Erlenmeyer flask 0.106g (1 mmol) of benzaldehyde and 0.108g (1 mmol) of phenylhydrazine were dissolved in 2 ml of dichloromethane. The reaction mixture was kept at room temperature for 10 minutes and then placed in a freezer (− 20 °C) for 30 minutes. During this period the product slowly crystallized from the mixture. The crystalline 1-benzylidene-2-phenylhydrazine was filtered and the product was air-dried for 12 hours. The purity was verified using GC-MS, LC-MS and NMR. Impurities were removed by recrystallization or preparative TLC to yield at least 98% purity product.

Synthesis of the substituted hydrazones—The above method was used for the synthesis of all other hydrazones studied in this work applying a variety of substituted hydrazines and benzaldehydes. The structure of the products was confirmed using mass spectrometry and ^{1}H, ^{19}F (when applicable), and ^{13}C NMR. The spectral data of the compounds are listed in the Supporting Information.

General Information - Biochemical assays

Sodium dihydrogenphosphate, disodium hydrogenphosphate, sodium azide, sodium hydroxide, sodium chloride, glycine, dimethylsulfoxide, and thioflavin-T were purchased

from Sigma-Aldrich. 1,1,1,3,3,3-Hexafluoro-2-propanol (HFIP), dimethylsulfoxide (DMSO), fluorescamine, ultrapure Tween 20, tetramethylbenzidine (free base), N,N-dimethylacetamide, tetrabutylammonium borohydride, and 30% (w/w) H_2O_2 were also obtained from Sigma–Aldrich. Lyophilized synthetic Aβ(1–40) and Aβ(1–42) peptides (purity>95%) and N-α- Biotinyl-Aβ(1–42) (bio-Aβ42) were AnaSpec products. Fatty acid-free fraction V bovine serum albumin was purchased from Boehringer–Mannheim. Streptavidin–HRP (SA–HRP) was a Rockland product. NeutrAvidin (NA) was obtained from Pierce. High-binding 9018 ELISA plates were purchased from Costar. The standards used in the SEC-HPLC investigations and the reference compounds (resveratrol and ascorbic acid) used in radical scavenging were purchased from Sigma-Aldrich. β-Nicotinamide-adenine-dinucleotide (NADH), phenazine methosulfate (PMS), and nitro-blue-tetrazolium (NBT) were VWR products while 2,2-di(4-tert-octylphenyl)-1-picrylhydrazine (DPPH) was obtained from Calbiochem.

Determination of inhibitor activity in Aβ fibrillogenesis and fibril disassembly by Thioflavin-T fluorescence assay

Inhibition of fibril formation: The assay was carried out using a standard published procedure.[35–37] The synthetic lyophilized Aβ(1–40) or Aβ(1–42) peptide was dissolved in 100 mM NaOH to a concentration of 40 mg/mL. This solution was diluted in 10 mM HEPES, 100 mM NaCl, 0.02% NaN_3 (pH=7.4) buffer to a final peptide concentration of 100 μM. The use of a strong base (NaOH) avoided the isoelectric point of Aβ, preventing low pH-assisted fibril or amorphous aggregate formation, providing the peptide in monomeric state.[38,39] The hydrazones were dissolved (10 mM) in dimethyl sulfoxide (DMSO) and were added to the Aβ samples in HEPES buffer in a molar ratio of inhibitor/Aβ=1 during the initial assays. This ratio was varied between 1 and 0.025 (1, 0.75, 0.5, 0.25, 0.125, 0.05, 0.025) during the EC_{50} determinations. The mixtures were vortexed for 30 s and the solutions were incubated at 37°C (77 rpm shaking) then samples were withdrawn for analysis after desired incubation time.

Disassembly of preformed fibrils [35]—Fibrils were grown as described above. The growth of the fibrils was followed by Thioflavin-T (THT) fluorescence measurements until the THT fluorescent intensity levelled off. The solution was then divided into aliquots for the disassembly studies. Ten millimolar stock compound solutions were prepared by dissolving the inhibitor compounds in DMSO; and this stock solution was added to the fibril samples to obtain 100 μM inhibitor concentration (1% DMSO) in the initial assays. For the EC_{50} determinations, the concentration of the test compounds was varied between 2.5 μM and 100 μM (inhibitor/Aβ molar ratios 1, 0.75, 0.5, 0.25, 0.125, 0.05, 0.025) while the peptide concentration was kept constant at 100 μM. After 30 s of vigorous vortexing, the solutions were re-incubated at 37°C with gentle shaking (77 rpm) and the decrease in fibril amount in each sample was measured after 4 days by THT fluorescence. To ensure that the inhibitors did not displace THT from the fibrils to decrease fluorescence intensity and thus causing false positive results, several experiments were carried out with compounds that showed significant inhibition of fibril formation or disassembly. Inhibitor-free Aβ control sample was labelled with THT and the fluorescence intensity was measured. Then an inhibitor (all compounds were tested separately) was added to the sample and the fluorescence measurement was repeated. No significant difference was obtained in the observed intensities indicating that the inhibitors did not affect the fluorescence assay.

THT fluorescence determination of the amount of fibrils[40–42]—The relative amount of fibrils was determined by Thioflavin-T fluorescence spectroscopy. The fluorescence intensities of the inhibitor-containing samples were compared to those without any inhibitor (control). The fluorescence measurements were carried out using a Hitachi

F-2500 fluorescence spectrophotometer. The incubated peptide solutions were briefly vortexed before each measurement, and then 3.5 μl aliquots of the suspended fibrils were withdrawn and added into 700 μL of 5 μM Thioflavin-T prepared freshly in 50 mM glycine-NaOH (pH=8.5) buffer. The maximum fluorescence intensity of these mixtures was measured at 484±5 nm emission wavelength with a preset excitation wavelength of 435 nm. None of the inhibitor compounds showed fluorescence intensity in this region. For the purposes of a screening assay, the fibril signal generated under the conditions of the assay in the presence of 1% DMSO (solvent control) and absence of compound is taken as 100%. The EC_{50} values of potent compounds were determined as described previously.[35,43]

Atomic Force Microscopy—The morphology of the incubated peptide samples were studied using atomic force microscopy (AFM) as described earlier.[43] 2 μL Aliquots were spotted on freshly cleaved mica sheets and air dried. The buffer salts were washed off with deionized water. The measuements were carried out using a Bruker-Innova SPM instrument.

Size exclusion chromatography[44]—Twenty μl of (day 0, 4, 6) samples were centrifuged at 16,100 × g = ~13,200 rpm (Eppendorf centrifuge: 5415D) for 35 minutes to sediment long insoluble fibrils and the supernatant stored at 4 °C between injections to slow down any further fibril growth. 10 μl of the supernatant was injected. Size exclusion chromatography was performed on HPLC system (Jasco PU-20895, quaternary gradient pump attached to Hewlett Packard Series 1050 UV detector) equipped with a TOSOH TSK-G3000SWXL column (30 cm × 7.8 mm ID, 5 μm particle size) with a separation range of 1–500 kDa (globular proteins). The mobile phase used was 0.1 M phosphate buffer (0.05% sodium azide and 0.1 M Na_2SO_4 at pH=6.7) to detect monomeric and oligomeric species. The flow rate was adjusted to 0.5 ml/min and the elution peaks were detected using UV-VIS detector at = λ254nm.

Determination of inhibitor activity in Aβ oligomer formation and oligomer disassembly by biotinyl-streptavidin assays[45,46]—Since Aβ(1–40) is the most abundant form of the peptide and readily forms fibrils it was decided to use it in the above assays. However, Aβ(1–42) was used for anti-oligomer assays because 1–40 forms oligomers poorly unless a stimulant is applied at the low peptide concentration (10 nM) used to avoid fibril formation.

Inhibition of Aβ oligomer assembly: Biotinyl-Aβ(1–42) stored as a 1 mg/mL solution in HFIP at −75 °C was dried with a nitrogen stream, treated with neat trifluoroacetic acid for 10 min at room temperature to disaggregate the peptide and dissolved to 500 nM (50×) in DMSO as described.[45,46] Two microliters of monomeric peptide was dispensed into each well of a polypropylene 96-well plate and 100 μL of PBS added containing the desired concentration of test compound and 1% DMSO to initiate oligomer formation at room temperature. After 30 min, 50 μL of 0.3% v/v Tween 20 was added to stop oligomer assembly. Fifty microliters of this mixture was then assayed for oligomer content by single-site Streptavidin-based assay.

Biotinyl-Aβ(1–42) single-site streptavidin-based assay for measurement of biotinyl-Aβ (1–42) oligomer content[45,46]: Fifty μl of 1 μg/mL NA in 10mM NaPi (pH=7.5) was coated per well overnight at 4 °C on Costar 9018 high-binding ELISA plates sealed with adhesive plastic film. The plates were blocked by the addition of 200 μl phosphate-buffered saline (PBS, 10mM sodium phosphate, 150mM NaCl [pH 7.5], 0.1%v/v Tween 20 at room temperature for 1–2 h and stored at 4 °C. After removal of the blocking solution, a sample containing a mixture of oligomers and monomers of biotinylated peptide (50 μl containing up to 10 nM biotinyl-Aβ) was allowed to bind for 2 h at room temperature. The wells were

washed three times with TBST (20mM Tris–HCl, 34mM NaCl [pH=7.5], and 0.1% v/v Tween 20) on a Biotek EL×50 automated plate washer. After washing, 50 μL of 1:20,000 SA–HRP in PBS + 0.1% v/v Tween 20 was added, the plate was sealed, and the incubation was continued for 1 h at room temperature. The plate was washed again with TBST, 100 μL of tetramethylbenzidine/H_2O_2 substrate solution was added, and the plate was incubated at room temperature for 5–10min. The OD_{450nm} was determined on a Biotech Synergy HT plate reader after stopping the reaction with 100 μl of 1% (v/v) H_2SO_4. For the purposes of a screening assay, the oligomer signal generated under the conditions of the assay in the presence of 1% DMSO (solvent control) and absence of compound was taken as 100%.

Assay for Aβ oligomer disassembly

Preparation of pre-formed biotinyl-Aβ(1–42) oligomers: Biotinyl-Aβ(1–42) was disaggregated as described for the assembly assay and DMSO added to the dried film to produce an 8 μg bio42/ml stock solution. After ten minutes the disaggregated peptide in DMSO was diluted 50-fold into PBS (20 mM sodium phosphate, 145 mM NaCl, pH 7.5) in a polypropylene container to 33.7 nM monomer (0.16 μg/ml). After one hour at room temperature an equal volume of PBS + 0.6% v/v Tween 20 was added to stop oligomer formation and stabilize the oligomers. This mixture of oligomeric and monomeric biotinyl-Aβ(1–42) was either used immediately or stored at −75 °C in polypropylene tubes up to six months. These oligomers are >70 kDa, and their size distribution by size exclusion chromatography is similar to that of Aβ oligomers from AD brain.[47]

Oligomer dissociation: Twenty-five microliters of 16.8 nM preformed bio42 oligomers in PBS + 0.3% Tween 20 were pipetted into wells of a polypropylene (wide well) 96-well plate (0.5 ml well capacity (Fisher 12565502) followed by 125 μl of PBS containing compound and 1 % v/v DMSO. The plate was sealed with a plastic sheet (Nunc 236366) and shaken (150 rpm) at room temperature for 16–18 hours. The amount of biotinyl-Aβ(1–42) oligomers remaining was measured by transferring 100 μl from each well to an NA-coated (50 ng/well) well of a Costar 9018 ELISA plate and quantified as described for oligomer assembly.

Determination of the antioxidant properties of the compounds

Scavenging of DPPH radical by the inhibitors[48]: A 2,2-diphenyl-picryl-hydrazyl radical (DPPH) stock solution was prepared in ethanol at 105.3 μM concentration. The test compound stock solutions were prepared by a co-solvent method to enhance solubility and keep the final DMSO concentration less than 0.1% in the assay. First, the compounds were dissolved in DMSO at 10 mM concentration then diluted with ethanol to 0.2 mM. Ninety five μL of the DPPH stock solution was dispensed into each well of a 96 well microplate and then 5 μL of the test compound stock solutions were added respectively. Thus, the final concentration of DPPH and test compounds in the assays was 100 μM and 10 μM, respectively. The plate was wrapped in aluminum foil and kept at 37 °C for 30 min. After incubation the decrease in DPPH absorption at 519 nm was measured by a Versamax microplate reader at 30 and 60 minutes. The % scavenging was calculated using the expression $[(Abs_c\text{-}Abs_{t.c})/Abs_c]*100$ where Abs_c is absorption of control sample that contained no inhibitor and $Abs_{t.c}$ is the absorption measured in the presence of the test compounds.

Scavenging of the superoxide radical by the inhibitors [49]: 1.5 mM β-Nicotinamide-adenine-dinucleotide (NADH), 0.03 mM phenazine methosulphate (PMS) and 0.375 mM nitro-blue-tetrazolium (NBT) solutions were prepared respectively in 100 mM phosphate buffer pH=7.4. The test compounds were dissolved in DMSO (10 mM). Ten μL of this compound solution was diluted with 74 μL of 100 mM phosphate buffer pH=7.4 and 76 μL

of acetonitrile to obtain a 0.625 mM solution containing less than 0.1% DMSO. One hundred seventy one μL of 100 mM phosphate buffer pH=7.4 was dispensed into each well of the microtiter plate along with 9 μL of 0.625 mM test compound solutions. Fifteen μL of 0.375 mM NBT and 15 μL of 1.5 mM NADH were rapidly added to each well. Lastly, 15 μL of 0.03 mM PMS solution was added to each well, except the blank. Final concentration of PMS, NBT, NADH and test compounds in the assay were 2 μM, 25 μM, 100 μM and 25 μM, respectively. The production of reduced NBT was monitored by a Versamax microplate reader at 560 nm. The absorbances were measured after 0, 1, 6, 8, 10, 12, 14 and 15 minutes.[49] The % superoxide scavenging activity was calculated using the expression $[(Abs_c\text{-}Abs_{t.c})/Abs_c]*100$ where Abs_c is absorption of sample that contained no inhibitor, and $Abs_{t.c}$ is the absorption measured in the presence of the test compounds.

RESULTS AND DISCUSSION

Design of the proposed bis(aryl)-hydrazone-based inhibitors

Resveratrol (Fig. 1), a natural product antioxidant, served as a starting point in our inhibitor design. This compound is commonly used in AD related studies as an Aβ self-assembly inhibitor as well as a radical scavenger.[29,30,50] Our proposed compounds are bis(aryl)-hydrazones that were inspired by the structure of resveratrol. Through systematic modification, their structure can readily be altered to fine tune their effects on Aβ assembly and antioxidant activity and possibly improve their pharmacokinetic properties. These compounds are likely antioxidants and could also affect π-π stacking interactions between Aβ units. The design of these compounds was based on the hypothesis that the tautomeric equilibrium between forms I and II (Fig. 1) would provide continuous conjugation and thus a nearly uniform π-electron delocalization for the compounds. The rapid tautomerism would result in an electronic structure (III) in which all three atoms (C-N-N) would be of at least partially sp^2 character and could contribute to a conjugated electron flow between the two aromatic rings. The general structure of the hydrazones and their similarity to resveratrol is illustrated in Fig. 1.

Based on the above reasoning a variety of bis(aryl)-hydrazones were synthesized from commercially available benzaldehydes and arylhydrazines. The basic synthetic procedure for preparation of these compounds is summarized in Fig. 2.

The starting materials for the synthesis were selected to ensure that hydrazones with varied substituents could be prepared. The aryl groups in the products possess either electron donating or electron withdrawing substituents, including fluorine-containing substituents that are commonly thought to increase the lipophilicity of the compounds.[51,52] A combinatorial approach was used to synthesize the compound library, possibly making every possible product from the building block pool. Overall, 44 compounds were synthesized. The general structure of the compounds is summarized in Fig. 3.

Effect of bis(aryl)-hydrazone-based inhibitors on Aβ self-assembly

After completion of the syntheses and structural validation the compounds were subjected to several biochemical assays. Due to the neurotoxicity associated with both the fibrillar aggregates and soluble oligomeric species these assays included tests to evaluate the inhibitory potential of the compounds in the self-assembly of the Aβ peptide (fibril and oligomer formation) as well as the disassembly of the preformed fibrils and oligomers. The well-known quantitative Thioflavin-T (THT) fluorescence spectroscopy assay was applied for the determination the antifibrillogenic activity of the compounds.[40–42] The calculated intensity values were based on the background (fluorescence of the THT alone) corrected maximum fluorescence intensities in the 480–490 nm region of the emission spectra after 4

days incubation. The measurements were made when the fibril assembly reached a plateau in the control sample. All data were normalized to inhibitor-free controls. These initial assays were carried out with Aβ:inhibitor=1 ratio at 100 μM Aβ concentration, thus the original inhibitor concentration was 100 μM. The compounds were also screened for anti-oligomer activity using the quantitative biotinyl-Aβ(1–42) single-site streptavidin-based assay,[45,46] at the initial Aβ:inhibitor= 0.0002 ratio at 0.01 μM biotinyl-Aβ(1–42) concentration (50 μM inhibitor concentration). The intensities of the inhibitor-containing samples (I_{sample}) were normalized to the control sample ($I_{control}$) containing Aβ and solvent control. The inhibition data expressed as percentile values with which a compound decreased the expected signal (control) are tabulated in Table 1:

$$\text{inhibition}(\%)=100-\frac{\text{I}_{\text{sample}}}{\text{I}_{\text{control}}}\times 100$$

In certain cases when compounds promoted the self assembly, $I_{sample} > I_{control}$; therefore negative inhibition percentile values were obtained.

After the quantitative THT-fluorescence assays, an independent method, Atomic Force Microscopy (AFM) was used to confirm the THT data and observe the morphology of the samples obtained with and without (control) hydrazones. Illustrative AFM images of a control sample and samples prepared in the presence of inhibitor and promoter compounds are depicted in Fig. 4

The AFM images are in good correlation with the THT fluorescence data (Table 1). The control sample (Fig. 4 Control) shows the expected, dense network of fibrils. Images obtained in the presence of compounds **1**, **3**, and **16**, respectively, indicate even more extensive fibril formation, very similar to that of the control. Considering that these compounds showed mild fibril-growth promoting effect (Table 1) the images are in agreement with the quantitative data. In contrast, compounds **13**, **19** and **35** visibly decreased the density of the fibrils and **37** resulted in an almost complete disappearance of fibrils. While similar fibrillar morphology was observed in the control and in samples with most compounds, **35** and **37** caused the formation of much shorter and non-uniform deposits, indicating the presence of protofibrils and amorphous protein deposits. This suggests that these compounds favored different pathways as compared to the unaltered control and most modulators or allowed the combination of pathways and remodeling.

Both Aβ(1–40) and Aβ(1–42) are found in fibrillar aggregates in the Alzheimer's disease brain.[1–3] Since Aβ(1–40) is the most abundant peptide and readily forms fibrils it was used in the fibrillogenesis assays. Aβ(1–42) was used for anti-oligomer assays because Aβ(1–40) forms oligomers poorly unless a stimulant, which introduces interpretation issues, is applied at the low peptide concentration (10 nM) used to avoid fibril formation. Since the two peptide variants may behave differently in the fibril formation assays, experiments were carried out with both peptides under identical conditions in the presence and absence of selected promoter and inhibitor compounds. Fibril growth was investigated as a function of time and expressed as the intensity of the measured fluorescence. The data are shown in Fig. 5.

The graphs are in agreement with previous observations of Aβ(1–40) and Aβ(1–42) fibril formation. The curves show that Aβ(1–40) fibril growth in the modulator-free sample (control) requires a longer time to reach maximum fluorescence (5 days) than Aβ(1–42), which displays a much faster initial rate reaching maximum fluorescence after 3 days. THT fluorescence decreases after the maximum I_{THT} values, most likely due to aging of separate

fibrils into bundles that either lose β-sheet structure or the THT cannot penetrate. The major differences between the two peptides are kinetic issues: Aβ(1–42) exhibits higher initial rate in fibrillogenesis, while Aβ(1–40) forms fibril bundles faster. Other than this the two peptides behaved similarly under our conditions. The addition of either promoters (**3**, **16**) or inhibitors (**35**, **37**) of fibril formation also affected the two peptides similarly. The percentile values of fibrillogenesis promotion/inhibition at the maximum of control (3 (Aβ(1–42)) vs. 5 days (Aβ(1–40))) and the shape of the curves are close, indicating that both Aβ variants behaved similarly under our assay conditions.

Many of the hydrazones possessed significant activity in fibrillogenesis inhibition and disassembly. Eleven compounds (**9–11, 13, 17–19, 35–38**) showed better than 50% activity in the fibril assembly inhibition and disassembly of preformed fibrils. A few compounds (**17, 37**) exhibited practically quantitative inhibition in these assays. However, the most pronounced effect was observed in inhibition of oligomer formation and disassembly of the preformed oligomers. Of the 43 compounds 30 showed better than 50% inhibition (36 showed better then 40%). Similar success rate was observed in the disassembly of the preformed oligomers. Many inhibitors (19 of the 43) completely disassembled (90–100%) the oligomers, while overall 22 compounds showed higher than 50% disassembly. The basic scaffold appears to be a suitable fit for inhibitor design, as a broad variety of hydrazones exhibited good to complete inhibitory activity in the initial assays.

Comparing the results in the above assays, the hydrazones commonly appear to act preferentially either as an anti-fibril agent or as an anti-oligomer agent. Compounds **1–8** demonstrate this very clearly, while nearly completely inhibiting oligomer formation they do not inhibit fibrillogenesis or even promote it. When compounds exhibit anti-fibril activity, they both inhibit assembly and promote disassembly. A similar phenomenon was observed with anti-oligomer compounds. This is consistent with general observations in the literature[10],[11] as well as our own recent work with organofluorine compounds.[43] Compounds **35, 36, 38, 43**, and **44** exhibited good to complete inhibition in all anti-fibril and anti-oligomer assays.

The data also indicated that 24 compounds (**1–7, 14–16, 22, 23, 25, 26, 30, 31, 33–36, 41–44**) appeared to be effective against oligomer assembly and in oligomer disassembly. Given the different time-frame of the assays (30 min for inhibition of oligomer assembly vs. overnight for disassembly) it is possible that certain compounds that are rapid disassembly agents would appear to be assembly inhibitors. To confirm whether the compounds are dual oligomer formation inhibitors and disassembly agents as opposed to rapid acting disassembly agents, short time dissociation assays were performed. These assays were run for 2h binding to the NA plate at 3 concentrations for each compound spanning the EC_{50}'s for the dissociation assay (50 μM, 25 μM and 12.5 μM). No dissociation was observed for those compounds during that period of time compared to a compound (2,5-dihydroxybenzoic acid) that is a rapid dissociator and does result in disassembly over that period of time.[44] These observations support the contention that the oligomer assembly inhibitors acted by inhibiting the formation of oligomers rather than acting as rapid dissociators in the assembly assay. Therefore the compounds listed above are dual assembly inhibitors and dissociators of Aβ(1–42) oligomers.

Compounds exhibiting greater than 50% inhibition in the screening assays were titrated to determine their EC_{50} values. The EC_{50} calculations followed a previously described method.[34,42] Fluorescence intensity vs. molar ratio functions were used to determine the relative potency of inhibitors similarly to the analysis of the Michaelis-Menten kinetics or ligand binding to macromolecules,[35,43]

$$I_{THT} = 100 - \frac{EC_{max}P}{EC_{50}+P}$$

, where I_{THT} is the fluorescence intensity of the inhibitor-containing sample (as % of control), P is the inhibitor/Aβ molar ratio, EC_{50} is the median inhibitor constant and EC_{max} is the maximum inhibition. The double reciprocal plot of the formula allowed the determination of EC_{50}. Since inhibitor/Aβ molar ratios (P) were applied in the formula, the EC_{50} values were obtained as a ratio as well. Multiplying this ratio by the Aβ concentration provided the values in concentration unit (μM). The EC_{50} values of the most active compounds obtained in the different assays are displayed in Table 2.

The data in Table 2 confirm the single concentration screening observations described above. The large proportion of highly active compounds indicate that the bis(aryl)-hydrazone skeleton is a promising scaffold for the synthesis of more potent Aβ self-assembly inhibitors. The overall activity of the compounds, in particular in oligomer-related assays are significant, the low micromolar EC_{50} values indicate that these compounds are potential leads for further inhibitor development. Most importantly three compounds (**34, 35** and **38**) interfered with both stages of Aβ assembly, desirably affecting all of the fibril/oligomer assembly/disassembly processes.

Considering the exceptionally complex nature of Aβ self-assembly and the possible stabilization formation of multiple intermediates e.g. neurotoxic oligomers, it is essential to know whether compounds stabilize soluble Aβ species in the process of inhibiting/reversing the formation of fibrils. For antifibrillogenic compounds whether the inhibitor halts the self-assembly at the Aβ monomer level or it allows the formation of soluble oligomers while preventing the formation of insoluble fibrils is of crucial importance. As the THT fluorescence detects and measures the insoluble fibrillar assemblies but not generally soluble oligomers, the supernatant of the selected samples, after centrifugation to remove large aggregates or fibrils, were subjected to size exclusion chromatography (SEC-HPLC) to determine the distribution of monomeric and oligomeric species that exist in the inhibited solutions.[44] One fibril promoter (**16**) and three inhibitors (**34, 36, 37**) were selected for these studies. The chromatograms including molecular weight calibration with globular proteins, are shown in Fig. 6.

The first (top) chromatogram clearly indicates the significant amount of soluble oligomers (both high and low molecular weight at ~11 and 16 min retention times) in the uninhibited control and the decreasing amount or complete lack of such species in the presence of the selected compounds. For example compound **34** appears to be one of the best oligomer inhibitors in the studied group based on the data shown in Tables 1 and 2. Accordingly, the chromatogram of the sample prepared with **34** shows minimal amount of soluble oligomeric species. For our purposes, these chromatograms suggest that while the compounds exhibit strong fibril inhibition they do not promote the formation or stabilization of oligomers. In certain cases, e.g. **37** the chromatogram indicates a relatively low peptide concentration. This suggests that a significant amount of peptide was removed during centrifugation. From the AFM image of the same sample (Fig. 4, **37**), sampled before centrifugation, the morphology of the peptide fibrils contained much shorter units as well as non-uniformly shaped, possibly amorphous, Aβ deposits as opposed to an extended fibrillar network (Fig. 4, control). These deposits are not fibrillar aggregates and do not fluoresce in the presence of THT. These observations explain the low fluorescence values obtained, as well as the low recovery of peptide observed in the SEC-HPLC chromatograms.

Antioxidant properties of bis(aryl)-hydrazones

Since the role of oxidative stress and harmful free radicals also appear important in the development of AD,[18–20] incorporating antioxidant properties in the design of anti-AD compounds could prove useful. Therefore, two commonly applied assays were used to evaluate the radical scavenging activity of the above mentioned hydrazones. One assay utilizes 2,2-diphenyl-1-picrylhydrazyl (DPPH), a stable free radical, and the reduction of free-radical concentration is measured directly by the absorbance of DPPH at λ=519 nm wavelength.[48] The other assay involves the generation of superoxide radicals in a nicotinamide adenine dinucleotide (NADH)/phenazinemethosulphate (PMS) system and the measurement of the absorbance of nitro blue tetrazolium (NBT), an indicator molecule that turns blue when reduced by superoxide. The free radical scavenging activity of the test compounds are determined by their ability to inhibit the reduction of NBT by superoxide.[49] The data, illustrated in Figs. 7 and 8, are compared to those obtained with reference compounds ascorbic acid[53] and resveratrol,[29,30,49] both of which are well-known antioxidants. All compounds were tested for their radical scavenging ability in these two assays.

In both assays the % reduction in the absorbance is directly proportional to the amount of free radical scavenged and serves as a quantitative measure of the anti-oxidant abilities. The hydrazone scaffold possesses significant antioxidant activity. In the DPPH scavenging assay ~ 30% of the compounds showed better or equal activity than either ascorbic acid or resveratrol. In several instances (**29, 30, 35**) the hydrazones scavenged over 65% of the radicals, twice the activity of the reference scavengers (ascorbic acid and resveratrol) at the same concentration (10 μM in DPPH and 25 μM in superoxide scavenging assays).

The hydrazones also exhibited activity against the superoxide radical. About 27% of the compounds possessed equal or higher activity than that of the reference compounds, moreover, three compounds (**19, 31, 41**) showed twice as high, and three compounds (**39, 40, 42**) over three fold the activity compared to ascorbic acid and resveratrol at the same concentration.

Conjugated electron structure and potentially oxidizable atoms are associated with strong antioxidant properties, characteristics that our hydrazones possess. As depicted in Fig. 1, the proposed tautomeric equilibrium via an 1,3-H-shift ensures that the compounds would have an extended largely delocalized electron structure and the N-atom is commonly observed to react with high energy oxygen species. While the activity of the compounds in the two radical scavenging assays generally correlate, few compounds that showed strong activity in the DPPH assay performed poorly in superoxide scavenging. Similarly, some strong superoxide scavengers exhibited only moderate activity against DPPH. The most likely explanation of this phenomenon lies in the significantly different size of the two radicals; the superoxide radical is small compared to the sterically bulky DPPH radical. As superoxide is the physiologically relevant radical, the superoxide scavenging is considered to be of primary importance. The extended conjugated electron structure could also contribute to the inhibition of the self-assembly of the Aβ peptide most likely through aromatic π- π interactions. The possible correlation between the radical scavenging effect and the self-assembly inhibition is unclear at this level of the research. While there are several hydrazones that are strong inhibitors as well as scavengers, there are compounds that show excellent inhibition but poor radical scavenging or strong radical scavenging but poor self-assembly inhibition. Thus, at present it appears that the radical scavenging and self-assembly activities are not linked together.

Nonetheless, in the studied set of compounds sharing the same core structure a variety of activities were found from self-assembly inhibitors to promoters. The significant changes in

the activity suggest that the substituents of the individual compounds have a significant effect on the overall characteristics of the hydrazones in the assays. Over the years a variety of compounds have been studied for their potential Aβ self-assembly inhibition properties.[4,7–13] Several recent papers were focused on the mechanism of action of selected examples.[54–59] While the primary goal of the current work is to identify hydrazone derivatives that are active against Aβ-self-assembly and can also scavenge free radicals, analyzing the structure-activity relationship of hydrazones could provide valuable information regarding drug-like properties or the mode of action of these compounds. The first important aspect that we considered was the hydrophobicity, which would primarily predict the potential bioavailability of the compounds and also affects their membrane permeability. Therefore, the log P values, commonly used to describe these features, were estimated using BioChemDraw (ver. 9.0, CambridgeSoft) (Table 1). It was observed that the log P of the hydrazones studied ranges from 2.33 to 5.17. According to the Lipinski rules[60] compounds with 2<log P< 5 are considered potentially bioavailable. Thus, while there are significant differences among the compounds, all can be considered to possess appropriate log P. Since the log P of the large majority of the above compounds possess falls within the 3–5 region, no clear relationship can be found between activity and hydrophobicity. Given the nature of the hydrazones (strongly basic compounds) and the assay conditions (slightly basic pH) the hydrazones will exist in their non-ionized, basic form thus, likely they will not act as surfactants.[54,56] If one considers the effect of substituents on the different activities several observations can be made, although an unambiguous conclusion cannot be drawn.

Compounds that possess H as R^2 group appear to act as strong fibrillogenesis promoters and excellent oligomer inhibitors (see **1–7, 14, 16**). As several other compounds with considerably small R^2 groups (e.g CF_3; **21, 22, 25, 28, 30, 31, 34–36**) exhibit strong oligomer inhibition, this phenomenon is probably linked to the size of the substituents, rather than their chemical nature. The same effect is even more pronounced for oligomer disassembly agents. A majority of the 19 compounds (**1–6, 14–16, 22, 25, 31, 33–36, 41, 43, 44**) that showed close to 100% disassembly in the initial assays (Table 1) has H as R^2 (11 of 19 compounds). This ratio increases to 16 of 19 compounds if one considers the also small CF_3 group as R^2. These compounds are either fibrillogenesis promoters or do not significantly affect the fibril formation. Thus, based on the above we can conclude that when small substituents (especially H) are in the R^2 position, then a potent selective anti-oligomer effect, both in assembly inhibition and oligomer disassembly, can be expected. On the other side of the scaffold, when R^1 is a strongly polar group, such as COOH or OH (e.g. **1, 21, 28, 31, 32, 41, 42**), the compound will most likely promote fibril formation. In contrast, many of the strong fibril inhibitors contain a NO_2 substituent, mostly in R^1.

Compounds with NO^2 and/or COOH groups dominate the strong superoxide scavengers. All hydrazones that exhibited > 25% superoxide scavenging (**10, 13, 19, 20, 31, 36, 39–42**) contain either NO2 or COOH or in a few cases both. Not surprisingly two of the three most active superoxide scavengers (scavenging>60%) (**39, 40**) possess both NO2 and COOH. The enhanced radical scavenging effect of these two groups can be explained by their delocalized electron structure fostering a stronger and further extended electron delocalization, a key factor in radical scavenging.

The above discussion indicates that the hydrazone scaffold serves as a useful foundation for the design of multifunctional anti-AD compounds. We showed that the substituents on this backbone play an important role in determining their activity in the different assays. More hydrazones with a broad group of substituents, including bulky (e.g. *t*-butyl or another ring) or electron donating ones (e.g. any alkyl), need to be tested to draw an accurate conclusion. In addition, the synthesis of further derivatives will be extended to aryl-alkyl (e.g.

acetophenones) and aryl-aryl (e.g. benzophenones) ketones to observe the effect of other groups connected to the chain.

CONCLUSIONS

The analysis of the above data indicates that the bis(aryl)-hydrazone skeleton is a promising scaffold for the design and synthesis of multifunctional compounds against Aβ self-assembly. Characteristically, the compounds in the synthesized hydrazone library exhibited strong activity either against fibril or oligomer formation as well as the disassembly of the preformed Aβ assemblies. This observation is in agreement with earlier suggestions that not all stable oligomers are obligatory precursors to the fibrils and that the two processes can occur in distinct pathways[10,11] as we have observed in previous investigations.[42]

However, a few compounds in our hydrazone library exhibited desirable effects against both fibril and oligomer self-assembly, as well as disassembling preformed fibrils and oligomers that form during Aβ self-assembly without stabilizing potentially toxic intermediates. Furthermore, about 30% of the studied hydrazones showed significant antioxidant behaviour, matching or surpassing the relevant activity of the well-known antioxidants ascorbic acid and resveratrol.

Based on the above investigations three compounds (**34, 35** and **38**) with combined Aβ self-assembly modulation and antioxidant activity were identified, providing promising starting points for more potent drug-like inhibitor design based on the hydrazone scaffold.

Supplementary Material

Refer to Web version on PubMed Central for supplementary material.

Acknowledgments

Financial support provided by the University of Massachusetts Boston, and National Institute of Health (R-15 AG025777-03A1 to B. T. and M. T.) and (R21AG028816-01 to H. L.) is gratefully acknowledged.

REFERENCES

1. Wetzel, R., editor. Methods in Enzymology. Academic Press; 1999. Amyloid, Prions, and Other Protein Aggregates; p. 309
2. Chiti F, Dobson CM. Amyloid formation by globular proteins under native conditions. Nat. Chem. Biol. 2008; 5:15–22. [PubMed: 19088715]
3. Walsh DM, Selkoe DJ. Aβ oligomers – a decade of discovery. J. Neurochem. 2007; 101:1172–1184. [PubMed: 17286590]
4. Estrada LD, Soto C. Disrupting beta-amyloid for Alzheimer's disease treatment. Curr. Top. Med. Chem. 2007; 7:115–126. [PubMed: 17266599]
5. Van der Schyf CJ, Mandel S, Geldenhuys WJ, Amit T, Avramovich Y, Zheng H, Fridkin M, Gal S, Weinreb O, Am OB, Sagi Y, Youdim MBH. Novel multifunctional anti-Alzheimer drugs with various CNS neurotransmitter targets and neuroprotective moieties. Curr. Alzheimer Res. 2007; 4:522–536. [PubMed: 18220515]
6. Cavalli A, Bolognesi ML, Capsoni S, Andrisano V, Bartolini M, Margotti E, Cattaneo A, Recanatini M, Melchiorre C. A small molecule targeting the multifactorial nature of Alzheimer's disease. Angew. Chem. Int. Ed. 2007; 46:3689–3692.
7. Stains C, Mondal K, Ghosh I. Molecules that target beta-amyloid. ChemMedChem. 2007; 2:1674–1692. [PubMed: 17952881]
8. Török B, Dasgupta S, Török M. Chemistry of small molecule inhibitors of Alzheimer's amyloid-beta fibrillogenesis. Curr. Bioact. Comp. 2008; 4:159–174.

9. Liu T, Bitan G. Modulating self-assembly of amyloidogenic proteins as a therapeutic approach for neurodegenerative diseases: Strategies and mechanisms. ChemMedChem. 2012; 7:359–374. [PubMed: 22323134]
10. Necula M, Kayed R, Milton S, Glabe CG. Small molecule inhibitors of aggregation indicate that amyloid β oligomerization and fibrillization pathways are independent and distinct. J. Biol. Chem. 2007; 282:10311–10324. [PubMed: 17284452]
11. Glabe CG. Structural classification of toxic amyloid oligomers. J. Biol. Chem. 2008; 283:29639–29643. [PubMed: 18723507]
12. Nerelius C, Johansson J, Sandegren A. Amyloid beta-peptide aggregation. What does it result in and how can it be prevented? Frontiers in Biosci. 2009; 14:1716–1729.
13. Sciaretta KL, Gordon DJ, Meredith SC. Peptide-based inhibitors of amyloid assembly. Method. Enzymol. 2006; 413:273–312.
14. Armstrong AH, Chen J, McKoy AF, Hecht MH. Mutations that replace aromatic side chains promote aggregation of the Alzheimer's Aβ peptide. Biochemistry. 2011; 50:4058–4067. [PubMed: 21513285]
15. Gazit E. Mechanisms of amyloid fibril self-assembly and inhibition. Model short peptides as a key research tool. FEBS J. 2005; 272:5971–5978. [PubMed: 16302962]
16. Gerrard JA, Hutton CA, Perugini MA. Inhibiting protein-protein interactions as an emerging paradigm for drug discovery. Mini Rev. Med. Chem. 2007; 7:151–157. [PubMed: 17305589]
17. LeVine H III. Small molecule inhibitors of Aβ-assembly. Amyloid. 2007; 14:185–197. [PubMed: 17701466]
18. Barnham KJ, Masters CL, Bush AI. Neurodegenerative diseases and oxidative stress. Nature Rev. 2004; 3:205–214.
19. Cavalli A, Bolognesi ML, Minarini A, Rosini M, Tumiatti V, Recanatini M, Melchiorre C. Multi-target-directed ligands to combat neurodegenerative diseases. J. Med. Chem. 2008; 51:347–372. [PubMed: 18181565]
20. DeToma SA, Choi J-S, Braymer JJ, Lim MH. Myricetin: A naturally occurring regulator of metal-induced amyloid-β aggregation and neurotoxicity. ChemBioChem. 2011; 12:1198–1201. [PubMed: 21538759]
21. Varadarajan S, Yatin S, Aksenova M, Butterfield DA. Review: Alzheimer's amyloid beta peptide-associated free radical oxidative stress and neurotoxicity. J. Struct. Biol. 2000; 130:184–208. [PubMed: 10940225]
22. Atwood CS, Obrenovich ME, Liu T, Chan H, Perry G, Smith MA, Martins RN. Amyloid-β: A chameleon walking in two worlds. A review of the trophic and toxic properties of amyloid-β. Brain Res. Rev. 2003; 43:1–16. [PubMed: 14499458]
23. Huang X, Moir RD, Tanzi RE, Bush AI, Rogers JT. Redox-active metals, oxidative stress, and Alzheimer's disease pathology. Ann. N Y Acad. Sci. USA. 2004; 1012:153–163.
24. Shoval H, Weiner L, Gazit E, Levy M, Pinchuk I, Lichtenberg D. Polyphenol-induced dissociation of various amyloid fibrils results in a methionine-independent formation of ROS. BBA-Proteins Proteom. 2008; 1784:1570–1577.
25. Baruch-Suchodolsky R, Fisher B. Aβ40 either soluble or aggregated, is a remarkably potent antioxidant in cell-free oxidative systems. Biochemistry. 2009; 48:4354–4370. [PubMed: 19320465]
26. Siegel SJ, Bieschke JE, Powers T, Kelly JW. The oxidative stress metabolite 4-hydroxynonenal promotes Alzheimer protofibril formation. Biochemistry. 2007; 46:1503–1510. [PubMed: 17279615]
27. Starkov AA, Beal FM. Portal to Alzheimer's disease. Nat. Med. 2008; 14:1020–1021. [PubMed: 18841137]
28. Shoval H, Lichhtenberg D, Gazit E. The molecular mechanisms of the anti-amyloid effects of phenols. Amyloid. 2007; 14:73–87. [PubMed: 17453627]
29. Rossi L, Mazzitelli S, Archiello M, Capo CR, Rotilio G. Benefits from dietary polyphenols for brain aging and Alzheimer's disease. Neurochem. Res. 2008; 33:2390–2400. [PubMed: 18415677]

30. Ono K, Condron MM, Ho L, Wang J, Zhao W, Pasinetti GM, Teplow DB. Effects of grape seed-derived polyphenols on amyloid beta-protein self-assembly and cytotoxicity. J. Biol. Chem. 2008; 283:32176–32187. [PubMed: 18815129]

31. Xu JZ, Yeung SY, Chang Q, Huang Y, Chen ZY. Comparison of antioxidant activity and bioavailability of tea epicatechins with their epimers. Br. J Nutr. 2004; 91:873–881. [PubMed: 15182391]

32. Rollas S, Küçükgüzel G. Biological activities of hydrazone derivatives. Molecules. 2007; 12:1910–1939. [PubMed: 17960096]

33. Gemma S, Colombo L, Forloni G, Savini L, Fracasso C, Caccia S, Salmona M, Brindisi M, Joshi V, Tripaldi P, Giorgi G, Taglialatela-Scafati O, Novellino E, Fiorini I, Campiani G, Butini S. Pyrroloquinoxaline hydrazones as fluorescent probes for amyloid fibrils. Org. Biomol. Chem. 2011; 9:5137–5148. [PubMed: 21629961]

34. Alptuzuen V, Prinz M, Horr V, Scheiber J, Radacki K, Fallarero A, Vuorela P, Engels B, Braunschweig H, Erciyas E, Holzgrabe U. Interaction of (benzylidene-hydrazono)-1,4-dihydropyridines with β-amyloid, acetylcholine, and butyrylcholine esterases. Bioorg. Med. Chem. 2010; 18:2049–2059. [PubMed: 20149667]

35. Török M, Abid M, Mhadgut SC, Török B. Organofluorine inhibitors of amyloid fibrillogenesis. Biochemistry. 2006; 45:5377–5383. [PubMed: 16618127]

36. Sood A, Abid M, Hailemichael S, Foster M, Török B, Török M. Effect of chirality of small molecule organofluorine inhibitors of amyloid self-assembly on inhibitor potency. Bioorg. Med. Chem. Lett. 2009; 19:6931–6934. [PubMed: 19880318]

37. Sood A, Abid M, Sauer C, Hailemichael S, Foster M, Török B, Török M. Disassembly of preformed amyloid beta fibrils by small organofluorine molecules. Bioorg. Med. Chem. Lett. 2011; 21:2044–2047. [PubMed: 21354796]

38. Fezoui Y, Hartley DM, Harper JD, Khurana R, Walsh DM, Condron MM, Selkoe DJ, Lansbury PT, Fink AL, Teplow DB. An improved method of preparing the amyloid beta-protein for fibrillogenesis and neurotoxicity experiments. Amyloid. 2000; 7:166–178. [PubMed: 11019857]

39. Bourhim M, Kruzel M, Srikrishnan T, Nicotera T. Linear quantitation of Aβ aggregation using Thioflavin T: Reduction in fibril formation by colostrinin. J. Neurosci. Methods. 2007; 160:264–268. [PubMed: 17049613]

40. Naiki H, Higuchi K, Hosokawa M, Takeda T. Fluorometric determination of amyloid fibrils in vitro using the fluorescent dye, thioflavine T. Anal. Biochem. 1989; 177:244–249. [PubMed: 2729542]

41. LeVine H III. Thioflavin T interaction with synthetic Alzheimer's disease β-amyloid peptides: Detection of amyloid aggregation in solution. Protein Sci. 1993; 2:404–410. [PubMed: 8453378]

42. Nilsson MR. Techniques to study amyloid fibril formation in vitro. Methods. 2004; 34:151–160. [PubMed: 15283924]

43. Török B, Sood A, Bag S, Kulkarni A, Borkin D, Lawler E, Dasgupta S, Landge SM, Abid M, Zhou W, Foster M, LeVine H III, Török M. Structure-activity relationship of organofluorine inhibitors of amyloid-beta self-assembly. ChemMedChem. 2012; 7:910–919. [PubMed: 22351619]

44. Walsh DM, Lomakin A, Benedek GB, Condron MM, Teplow DB. Amyloid beta-protein fibrillogenesis - Detection of a protofibrillar intermediate. J. Biol. Chem. 1997; 272:22364–22372. [PubMed: 9268388]

45. LeVine H III. Biotin-avidin interaction-based screening assay for Alzheimer's β-peptide oligomer inhibitors. Anal. Biochem. 2006; 356:265–272. [PubMed: 16729955]

46. LeVine H III, Ding Q, Walker JA, Voss RS, Augelli-Szafran CE. Clioquinol and other hydroxyquinoline derivatives inhibit Aβ(1–42) oligomer assembly. Neurosci. Lett. 2009; 465:99–103. [PubMed: 19664688]

47. LeVine H III. Alzheimer's beta-peptide oligomer formation at physiologic concentrations. Anal. Biochem. 2004; 335:81–90. [PubMed: 15519574]

48. (a) Huang D, Ou B, Prior RL. The chemistry behind antioxidant capacity assays. J. Agric. Food Chem. 2005; 53:1841–1856. [PubMed: 15769103] (b) Sanchez-Moreno C. Review: Methods used to evaluate the free radical scavenging activity in foods and biological systems. Food Sci. Technol.

Int. 2002; 8:121–129.(c) Brand-Williams W, Cuvelier ME, Berset C. Use of a free radical method to evaluate antioxidant activity. Lebensm.-Wiss. u.-Technol. 1995; 28:25–30.

49. Liu F, Ooi VEC, Change ST. Free radical scavenging activity of mushroom polysaccharide extracts. Life Sci. 1997; 60:763–771. [PubMed: 9064481]
50. Delmas D, Aires V, Limagne E, Dutartre P, Mazue F, Ghiringhelli F, Latruffe N. Transport, stability, and biological activity of resveratrol. Ann. N.Y. Acad. Sci. 2011; 1215:48–59. [PubMed: 21261641]
51. Hiyama, T., editor. Organofluorine Compounds. Berlin: Springer; 2000.
52. Ojima, I.; McCarthy, JR.; Welch, JT., editors. Biomedical Frontiers of Fluorine Chemistry. Washington, DC: American Chemical Society; 1996.
53. Balsano C, Alisi A. Antioxidant effects of natural bioactive compounds. Current Pharmaceut. Design. 2009; 15:3063–3073.
54. Feng BI, Toyama BH, Wille H, Colby DW, Collins SR, May BCH, Prusiner SB, Weissman J, Shoichet BK. Small-molecule aggregates inhibit amyloid polymerization. Nature Chem. Biol. 2008; 4:197–199. [PubMed: 18223646]
55. Lendel C, Bertoncini CW, Cremades N, Waudby CA, Vendruscolo M, Dobson CM, Schenk D, Christodoulou J, Toth G. On the mechanism of nonspecific inhibitors of protein aggregation: Dissecting the interactions of α-synuclein with congo red and lacmoid. Biochemistry. 2009; 48:8322–8334. [PubMed: 19645507]
56. Lendel C, Bolognesi B, Wahlström A, Dobson CM, Gräslund A. Detergent-like Interaction of Congo Red with the Amyloid β Peptide. Biochemistry. 2010; 49:1358–1360. [PubMed: 20070125]
57. Lamberto GR, Torres-Monserrat V, Bertoncini CW, Salvatella X, Zweckstetter M, Griesinger C, Fernandez C. Toward the discovery of effective polycyclic inhibitors of α- synuclein amyloid assembly. J. Biol. Chem. 2011; 286:32036–32044. [PubMed: 21795682]
58. Ryan TM, Griffin MDW, Teoh CL, Ooi J, Howlett GJ. High-affinity amphipathic modulators of amyloid fibril nucleation and elongation. J. Mol. Biol. 2011; 406:416–429. [PubMed: 21185302]
59. Abelein A, Bolognesi B, Dobson CM, Graslund A, Lendel C. Hydrophobicity and conformational change as mechanistic determinants for nonspecific modulators of amyloid β self-assembly. Biochemistry. 2012; 51:126–137. [PubMed: 22133042]
60. Lipinski CA, Lombardo F, Dominy BW, Feeney PJ. Experimental and computational approaches to estimate solubility and permeability in drug discovery and development settings. Adv. Drug Delivery Rev. 1997; 23:3–25.

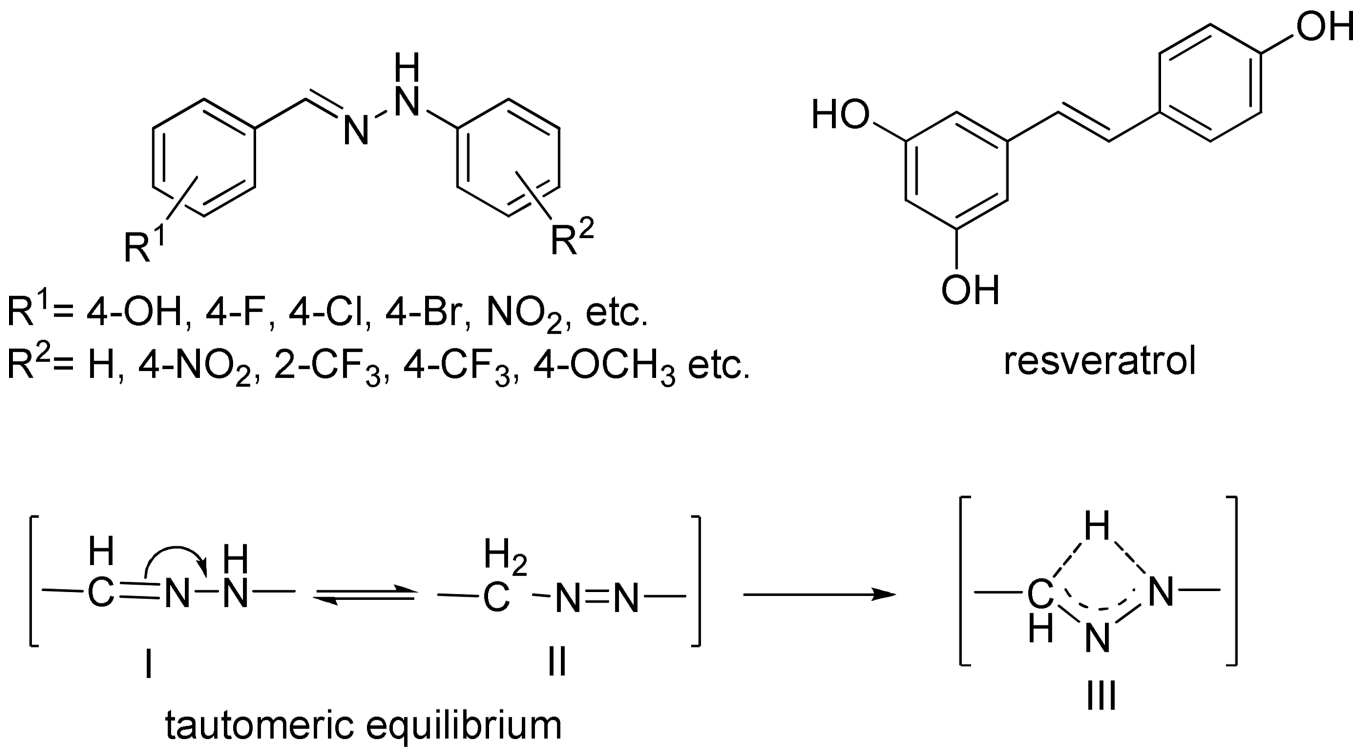

Figure 1.
General structures of hydrazones and resveratrol

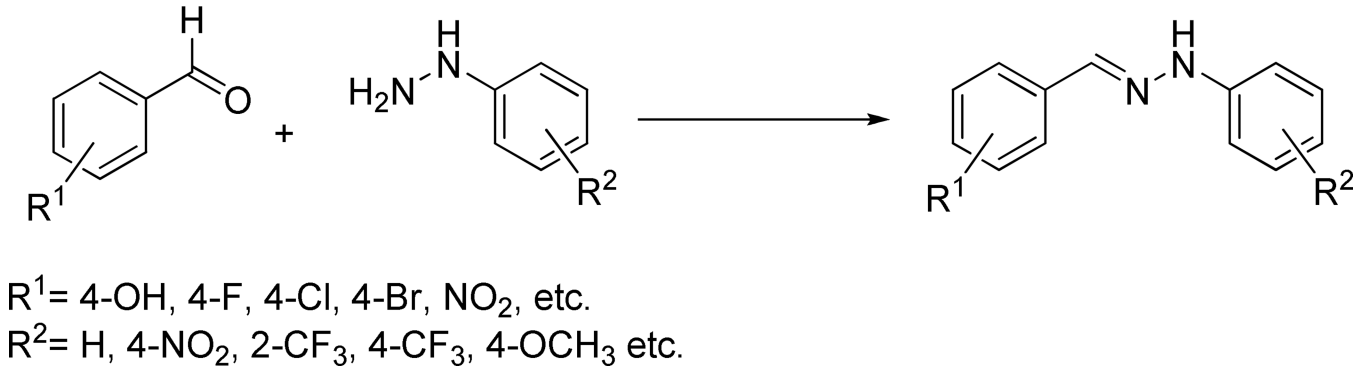

R^1= 4-OH, 4-F, 4-Cl, 4-Br, NO_2, etc.
R^2= H, 4-NO_2, 2-CF_3, 4-CF_3, 4-OCH_3 etc.

Figure 2.
Synthesis of diaryl-hydrazones

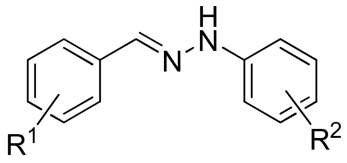

	R^1	R^2
1	4-OH	H
2	3,4-diOCH_3	H
3	4-Br	H
4	4-Cl	H
5	4-F	H
6	3-Cl	H
7	4-CN	H
8	4-NO_2	2-CF_3
9	4-NO_2	4-NO_2
10	4-NO_2	3-CF_3
11	4-NO_2	4-CF_3
12	4-NO_2	2-Pyrrolyl
13	4-NO_2	2-Bz
14	2-Br	H
15	3-CF_3	H
16	4-CF_3	H
17	4-OH	4-NO_2
18	4-CF_3	4-NO_2
19	3,4-diOCH_3	4-NO_2
20	2-Br	4-NO_2
21	4-OH	2-CF_3
22	3,4-diOCH_3	2-CF_3
23	2-Br	2-CF_3
24	4-CF_3	2-CF_3
25	2-Br	3-CF_3
26	2-Br	2-CF_3
27	2-OH-4-OCH_3	4-CF_3
28*	2-COOH	3-CF_3
29	4-N,N-diCH_3	2-CF_3
30	4-N,N-diCH_3	3-CF_3
31*	2-COOH	4-CF_3
32	2-OH-4-OCH_3	3-CF_3
33	4-OBn	H
34	4-N,N-diCH_3	4-CF_3
35	4-N,N-diCH_3	4-OCH_3
36	4-N,N-diCH_3	4-NO_2
37	2-Pyrrolyl	4-CF_3
38	4-NO_2	H
39	4-COOH	2-NO_2
40	4-COOH	4-NO_2
41	4-COOH	4-OCH_3
42	4-COOH	4-CF_3
43	4-OCH_2CH_2OH	4-CF_3
44	H	H

* Due to the close proximity of the 2-COOH (R^1) to the NH, these compounds formed a cyclic structure below:

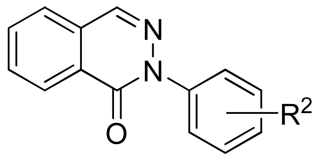

Figure 3.
Structure of diaryl-hydrazones used in this study

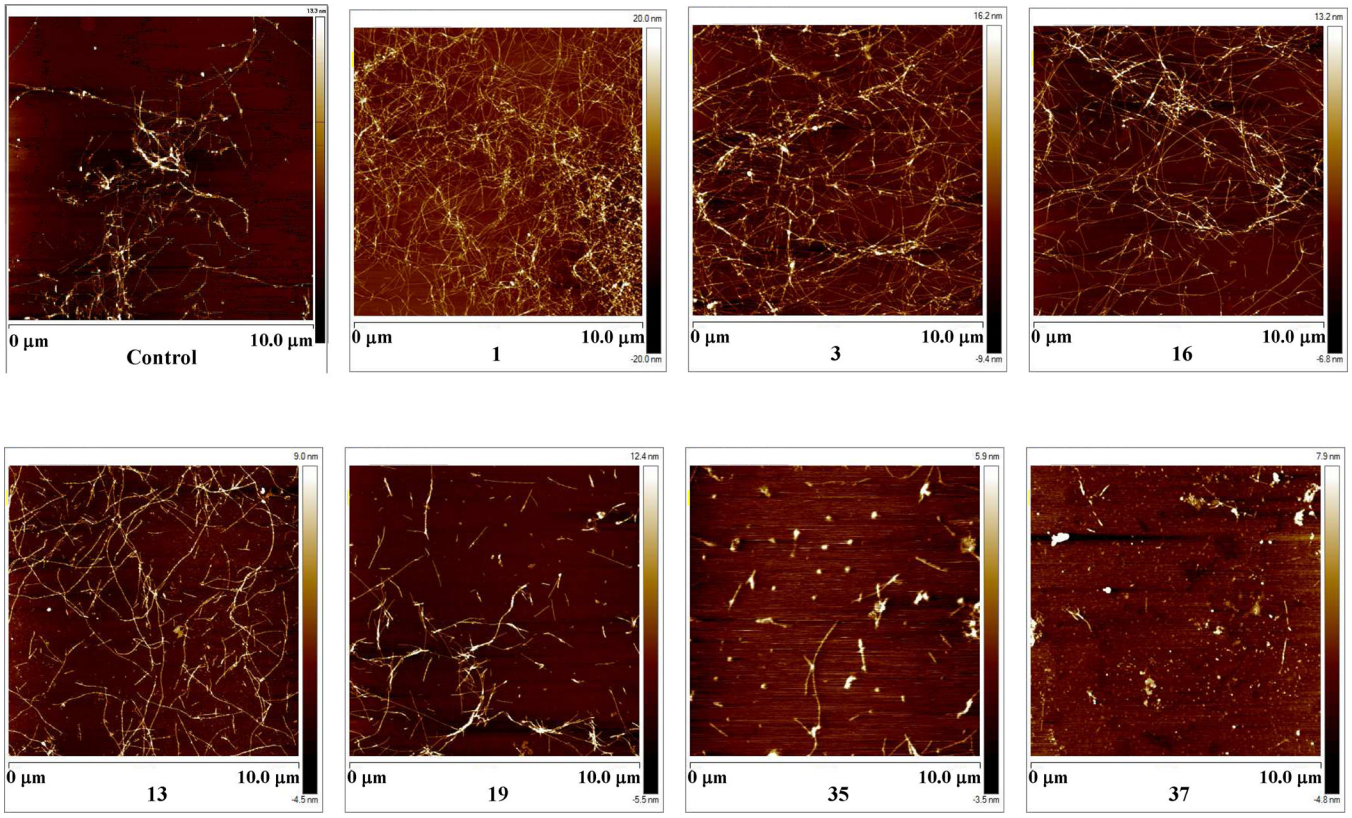

Figure 4.

Atomic Force Microscopy images of $A\beta_{1-40}$ samples incubated without (control) and with the affector compounds for 6 days. The compounds numbers denote the inhibitor compounds as they are shown in Fig. 3.

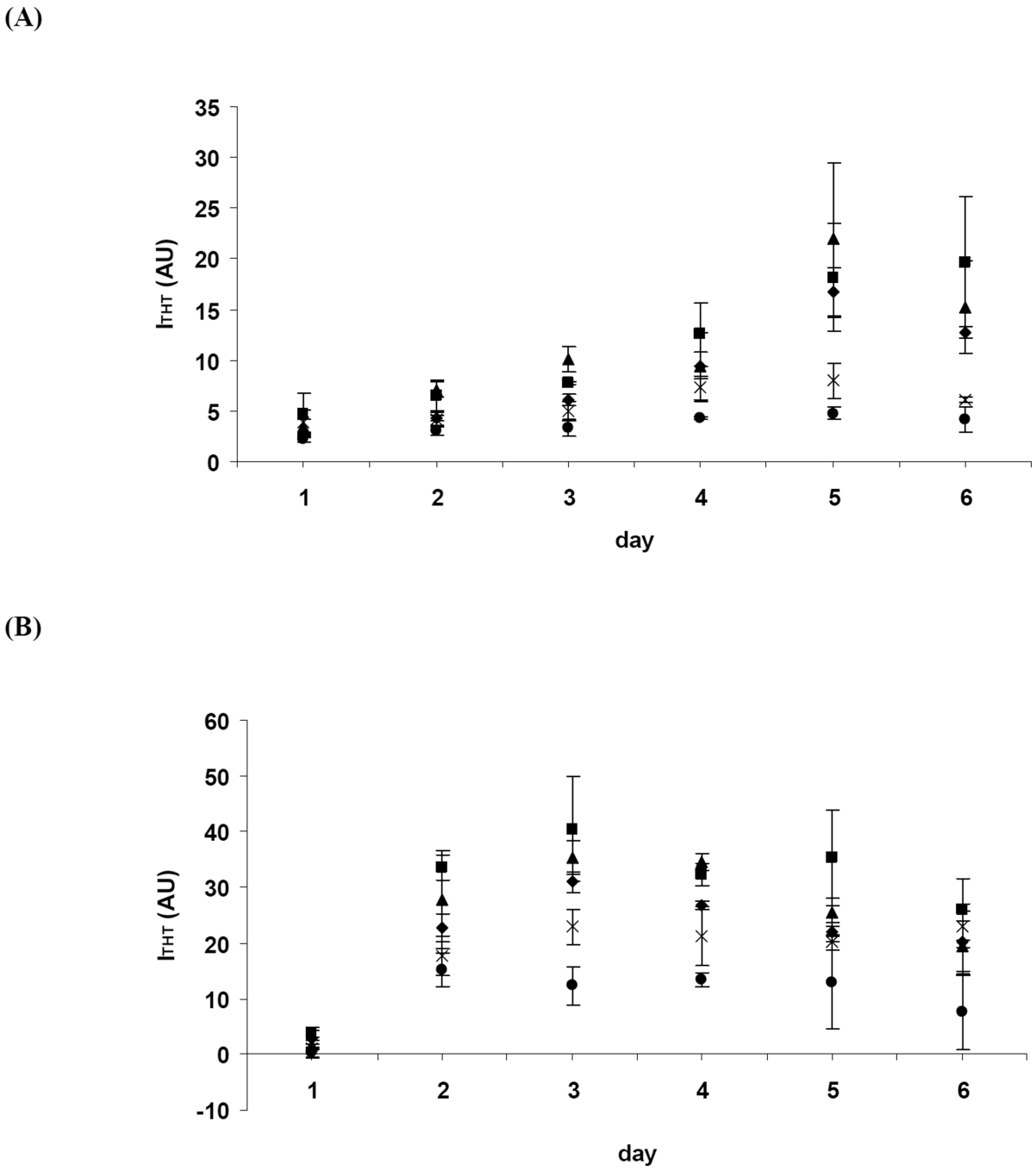

Figure 5.

The effect of incubation time on the amount of fibrils formed (expressed as fluorescence intensity, I_{THT}) in (A) $A\beta_{1-40}$ and (B) $A\beta_{1-42}$ samples incubated without (control) and with the affector compounds for 6 days. The compounds numbers denote the inhibitor compounds as they are shown in Fig. 3 (♦ - control; in the presence of compound: ■ – **3**; ▲ – **16**; X – **35**; ● – **37**) The values represent means±standard deviation of the data (n=3)

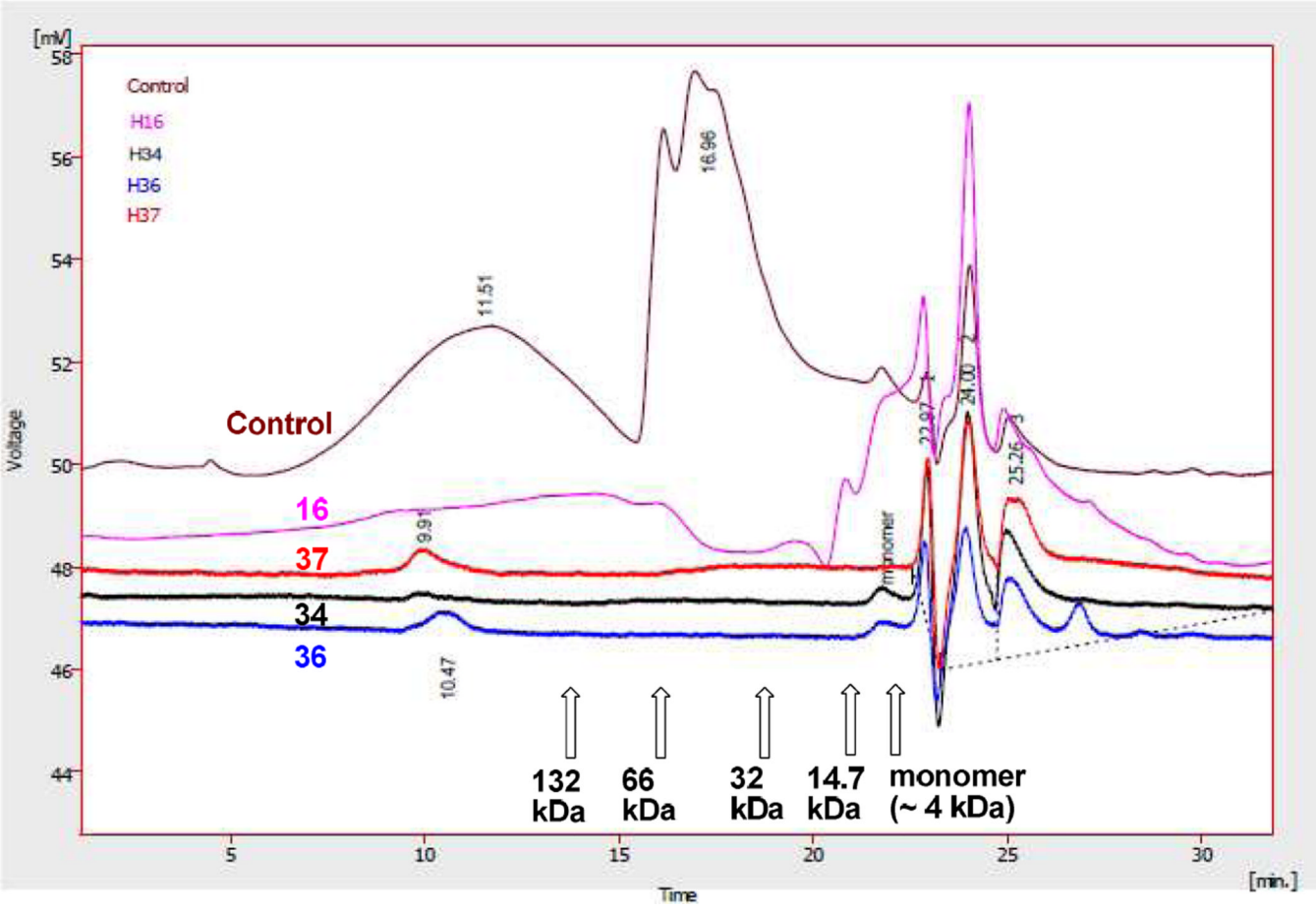

Figure 6.

TSK G3000SWXL SEC-HPLC chromatograms of Aβ samples after centrifugation at 16, 100 xg (to remove fibrils) with/without selected hydrazone inhibitors. The compound numbers refer to structures shown in Fig. 3/Table 1. The molecular weight globular protein standards used to calibrate the column elution profile were β-galactosidase (132 kDa), bovine serum albumin (66 kDa), superoxide dismutase (32 kDa) and lysozyme (14.7 kDa). The intense peaks at ~24 min represent DMSO used as solvent during the preparation of the inhibitor solutions.

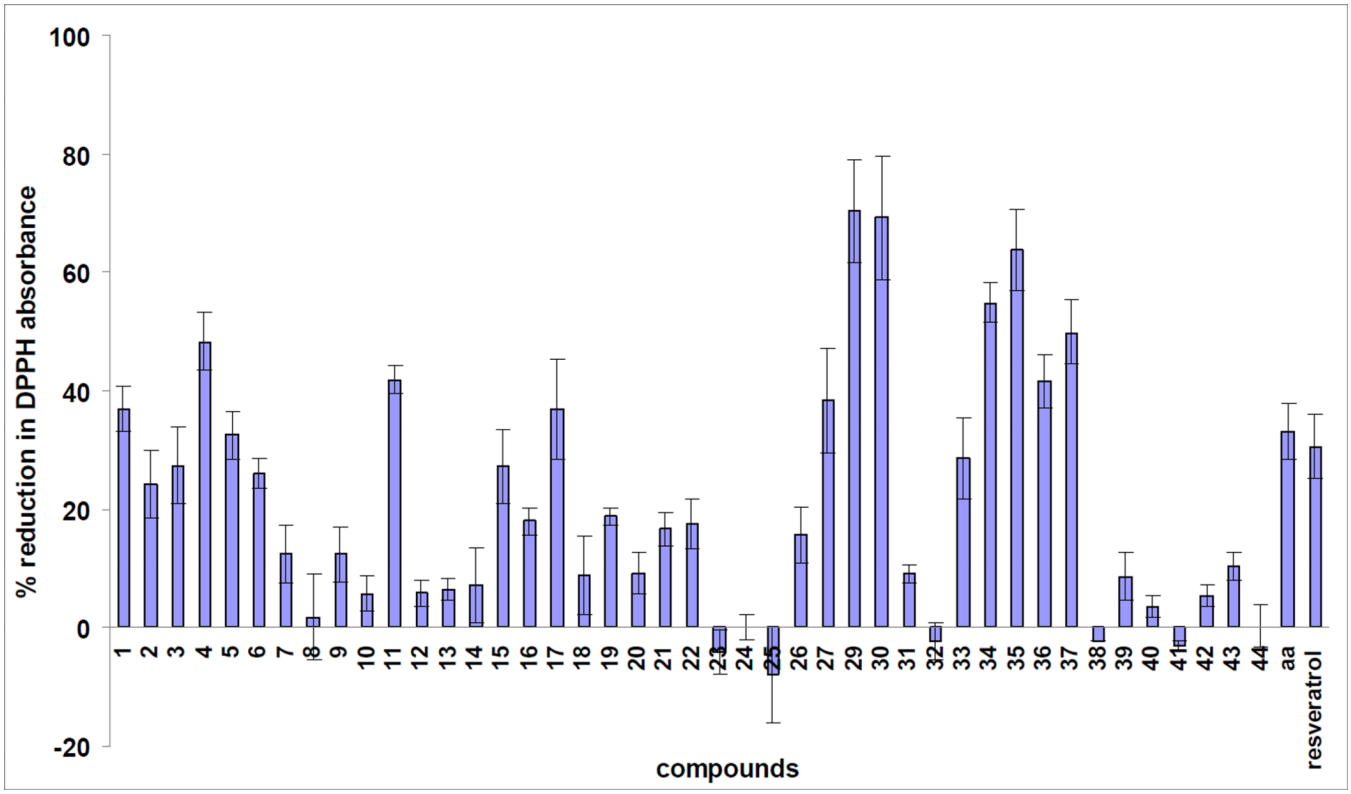

Figure 7.

Radical scavenging activity of selected hydrazones (activity > 10%) illustrated as % reduction of the absorbance of DPPH at λ=519 nm after 60 min incubation. The compound numbers refer to structures shown in Fig. 3 and Table 1. Ascorbic acid (aa) and resveratrol were used as reference compounds. The values represent means ± standard deviation of the data (n=3–4).

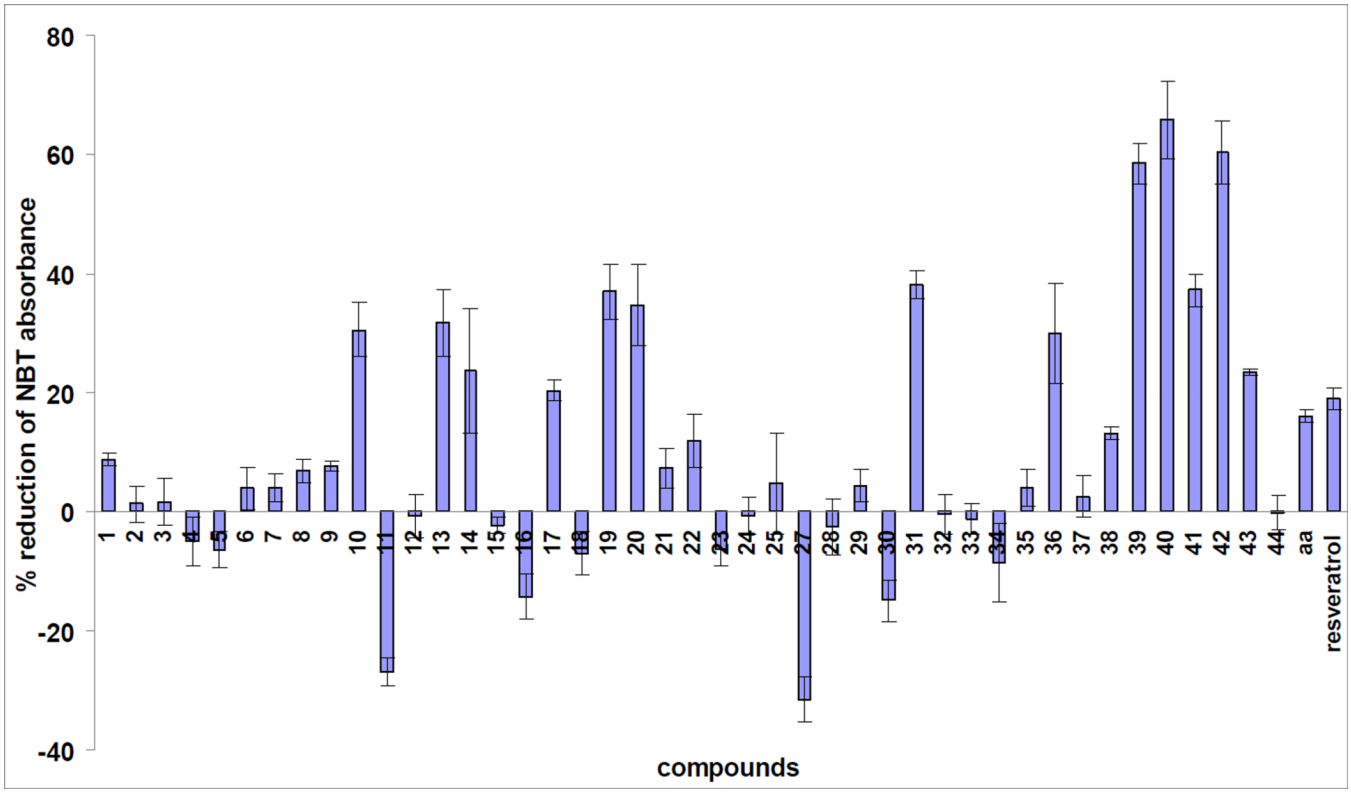

Figure 8.

Superoxide scavenging activity of selected hydrazones (activity > 2%) illustrated as % reduction of the absorbance of NBT at λ=560 nm after 10 min incubation. The compound numbers refer to structures shown in Fig. 3 and Table 1. Ascorbic acid (aa) and resveratrol were used as reference compounds. The values represent means ± standard deviation of the data (n=3–4).

Table 1

Inhibition of the Aβ self-assembly by the diaryl-hydrazones[a–e]

Compound	log P	$\text{Inhibition}_{\text{fibril}}$[a] (%)	$\text{Disassembly}_{\text{fibril}}$[b] (%)	$\text{Inhibition}_{\text{oligomer}}$[c] (%)	$\text{Disassembly}_{\text{oligomer}}$[d] (%)
1	3.03	−37 ± 24.6	48 ± 1.7	98 ± 1.5	100 ± 0.5
2	3.16	20 ± 12.3	35 ± 1.7	100 ± 0.2	100 ± 2.3
3	4.25	−21 ± 16.0	21 ± 16.0	93 ± 1.0	100 ± 0.9
4	3.98	−34 ± 17.3	28 ± 7.2	95 ± 0.8	100 ± 0.2
5	3.58	−12 ± 15.4	33 ± 7.7	97 ± 1.0	100 ± 0.6
6	3.98	33 ± 29.8	31 ± 3.7	96 ± 0.5	100 ± 0.2
7	3.45	−38 ± 20.6	22 ± 19.0	84 ± 4.2	42 ± 6.8
8	4.50	-	33 ± 8.3	95 ± 1.6	4 ± 9.3
9	3.48	52 ± 11.8	41 ± 15.2	76 ± 6.6	6 ± 6.5
10	4.50	53 ± 16.0	56 ± 11.1	27 ± 5.1	3 ± 11.1
11	4.50	83 ± 0.8	63 ± 11.8	34 ± 15.8	0 ± 5.2
12	2.33	23 ± 9.8	55 ± 4.3	43 ± 8.2	19 ± 7.6
13	3.40	54 ± 30.2	26 ± 16.4	-	-
14	4.25	−8.2 ± 32.9	−12 ± 11.6	88 ± 6.7	99 ± 2.3
15	4.34	16 ± 7.6	−16 ± 15.2	98 ± 4.1	95 ± 3.9
16	4.34	−26 ± 18.6	−14 ± 16.4	93 ± 0.2	99 ± 0.3
17	3.13	87 ± 28.7	91 ± 4.2	13 ± 10.2	−15 ± 4.6
18	4.50	56 ± 18.8	12 ± 11.0	75 ± 8.2	−16 ± 7.8
19	3.78	54 ± 18.6	59 ± 2.1	7 ± 8.8	−15 ± 5.6
20	4.41	39 ± 31.6	27 ± 10.8	100 ± 1.1	0 ± 7.8
21	3.95	−18.7 ± 85.0	17 ± 2.9	55 ± 14.2	17 ± 2.9
22	4.09	−17 ± 10.5	27 ± 1.4	82 ± 2.5	91 ± 1.9
23	5.17	37 ± 1.5	34 ± 15.4	32 ± 9.3	54 ± 12.5
24	5.26	−31 ± 25.9	29 ± 14.0	43 ± 7.4	16 ± 5.4
25	5.17	3 ± 40.0	20 ± 8.2	99 ± 0.8	100 ± 0.4
26	5.17	−32 ± 27.0	27 ± 6.2	41 ± 6.4	31 ± 6.4
27	3.82	14 ± 15.4	47 ± 5.7	28 ± 5.0	−5 ± 1.6
28	4.15	−50 ± 9.6	-	73 ± 6.8	−11 ± 2.9

Compound	log P	Inhibition$_{fibril}$[a] (%)	Disassembly$_{fibril}$[b] (%)	Inhibition$_{oligomer}$[c] (%)	Disassembly$_{oligomer}$[d] (%)
29	5.11	−28 ± 26.8	44 ± 16.1	31 ± 14.1	−4 ± 4.5
30	5.11	10 ± 9.8	41 ± 10.5	60 ± 48.5	23 ± 5.8
31	4.15	−46 ± 13.3	40 ± 15.3	85 ± 1.5	100 ± 0.1
32	3.82	−29 ± 30.5	−8 ± 49.8	4 ± 0.6	10 ± 0.8
33	5.02	21 ± 17.0	59 ± 4.6	57 ± 18.9	100 ± 0.4
34	4.62	38 ± 33.7	1 ± 11.1	80 ± 6.3	98 ± 2.3
35	3.58	63 ± 12.9	75 ± 1.5	87 ± 1.4	97 ± 0.7
36	4.36	53 ± 29.5	24 ± 7.8	89 ± 2.0	98 ± 0.7
37	2.88	81 ± 19.3	99 ± 1.4	−25 ± 40.3	−13 ± 6.2
38	3.52	78 ± 0.7	75 ± 4.0	72 ± 7.1	15 ± 14.7
39	2.88	41 ± 16.8	41 ± 1.0	47 ± 14.2	11 ± 1.8
40	2.88	37 ± 5.4	50 ± 11.9	36 ± 15.3	4 ± 3.9
41	2.85	−43 ± 17.7	45 ± 17.8	100 ± 1.1	96 ± 0.4
42	3.90	−18 ± 3.9	23 ± 17.3	64 ± 16.6	57 ± 1.5
43	3.70	19 ± 17.2	63 ± 8.2	53 ± 28.0	97 ± 0.7
44	3.42	15 ± 0.2	55 ± 18.2	96 ± 3.7	100 ± 0.5

[a] inhibition of the Aβ fibrillogenesis by the compound at an inhibitor: Aβ=1 ratio; 100 μM Aβ concentration

[b] disassembly of preformed Aβ fibrills by the compound at an inhibitor: Aβ=1 ratio; 100 μM Aβ concentration

[c] inhibition of the Aβ oligomer formation by the compound at Aβ:inhibitor= 0.0002; Aβ 10 nM concentration

[d] disassembly of preformed Aβ oligomers by the compound at Aβ:inhibitor= 0.0002; Aβ 10 nM concentration

[e] The values represent means ± standard deviation of the data (n=2–7)

Table 2

EC_{50} values of selected bis(aryl)-hydrazones in the inhibition of Aβ self-assembly[a]

Compound	log P	$EC_{50\text{-}F}$[b] (μM)	$EC_{50\text{-}DF}$[c] (μM)	$EC_{50\text{-}O}$[d] (μM)	$EC_{50\text{-}DO}$[e] (μM)
1	3.03	-	-	10.6	21
2	3.16	-	-	6.5	3
3	4.25	-	-	5.4	7
4	3.98	-	-	5.4	6.4
5	3.58	-	-	7	5.2
6	3.98	-	-	3.6	7.3
7	3.45	-	-	18	36
8	4.50	-	-	20	-
9	3.48	16	-	80	-
10	4.50	68	-	90	-
11	4.50	33	-	54	-
12	2.33	-	-	43	-
14	4.25	-	-	4.7	2.3
15	4.34	-	-	5.8	14.5
16	4.34	-	-	7.8	12.5
17	3.13	10	62.5	-	-
18	4.50	-	-	34	-
19	3.78	80	-	-	-
20	4.41	-	-	5	-
22	4.09	-	-	39	22
23	5.17	-	-	58	32
25	5.17	-	-	2.4	6.3
27	3.82	43	-	-	-
28	4.15	-	-	36	-
31	4.15	-	-	-	7.7
33	5.02	-	-	1.8	2.1
34	4.62	95	-	1.4	2.1
35	3.58	15	64	22	12

Compound	log P	$EC_{50\text{-}F}$[b] (μM)	$EC_{50\text{-}DF}$[c] (μM)	$EC_{50\text{-}O}$[d] (μM)	$EC_{50\text{-}DO}$[e] (μM)
36	4.36	-	-	17	11
37	2.88	30	-	-	-
38	3.52	14	-	24	45
41	2.85	-	-	7.4	4.6
43	3.70	-	95	60	8
44	3.42	-	-	6.6	5.4

[a] Dashes indicate no inhibition or EC_{50} > 100 μM for fibril inhibition and no inhibition or EC_{50} > 50μM for oligomer inhibition.

[b] $EC_{50\text{-}F}$: EC_{50} value of the inhibition of the Aβ fibrillogenesis

[c] $EC_{50\text{-}DF}$: EC_{50} value of the disassembly of preformed Aβ fibrils

[d] $EC_{50\text{-}O}$: EC_{50} value of the inhibition of the Aβ oligomer formation

[e] $EC_{50\text{-}DO}$: EC_{50} value of the disassembly of preformed Aβ oligomers